

# The Brittle Fracture of Tempered Glass and its Relation to the Occurrence of Earthquakes,?

著者	Suzuki Ziro, Hamaguchi Hiroyuki
雑誌名	Science reports of the Tohoku University. Ser. 5, Geophysics
巻	18
号	1
ページ	16-39
発行年	1966-07
URL	<a href="http://hdl.handle.net/10097/44678">http://hdl.handle.net/10097/44678</a>

# *The Brittle Fracture of Tempered Glass and its Relation to the Occurrence of Earthquakes, I*

ZIRO SUZUKI and HIROYUKI HAMAGUCHI

Geophysical Institute, Tohoku University, Sendai, Japan

(Received May 23, 1966)

**Abstract:** An experiment on secondary microfractures in tempered glass is carried out in special reference to the statistical properties of aftershocks. If a tempered glass or prestressed glass is fractured, many secondary microfractures follow the main fracture without additive force. These secondary fractures last for several hours at the most. Three kinds of tempered glasses, which are provisionally called high, medium and low state, according to the pre-existing stress are adopted as material. Sound waves generated by these fractures are detected by a microphone connected with tape recorder and their magnitude and time distributions are studied comparing with those for actual earthquakes.

The magnitude distribution of secondary fractures are not always represented by the so-called Ishimoto-Iida's relation (or Gutenberg-Richter's relation), which is valid in most cases of earthquakes. The frequency distribution of amplitudes shows a sudden decrease (cut-off) in a larger side of amplitude, while it is well expressed by a straight line on a doubly logarithmic diagram in a smaller amplitude side.

The cut-off amplitude is closely related with the magnitude of stress which was stored in the material before fracture. The larger stress indicates the smaller cut-off amplitude. Since this sort of cut-off is seldom found in actual earthquakes, the seismic area corresponds to the lower state of stress accumulation than that of low stress specimen in our experiment.

When the stress is high and the cut-off is clearly seen, it is found that the course of occurrence of secondary fractures can be divided into two stages based on the energy release with respect to time. The Ishimoto-Iida's relation holds good in the earlier stage irrespective of stored stress, while the relation is disturbed in the later stage in the cases of high and medium stress states.

Time distribution is well expressed by the generalized Omori's formula with respect to time lapse. The value of parameter  $p$  in the formula changes with stored stress so that the smaller  $p$  appears in the higher state. The values obtained in this experiment are smaller than those for aftershocks even in the case of low stress stage. This implies that the actual seismic area corresponds to the lower accumulation of stress than the low state of the used glass.

Pattern of fracture is also an interesting feature in relation to the stored stress and the method of initiation of main fracture. Some discussions on the results are made in reference to the studies for natural earthquakes.

## 1. Introduction

A number of studies have been made in the field of statistical seismology and some important relations have been established concerning various natures of earthquakes. For example, Gutenberg and Richter (1949) found the famous magnitude distribution for large earthquakes. Suzuki (1959) and many other Japanese seismologists established that the same relation holds down to microearthquakes having the magnitude of 0 or less. Time and space distributions of earthquakes are also minutely studied by many

authors, and the functional form of these distributions, as well as the numerical values of parameters, is obtained. Various statistical investigations have been made on aftershocks, especially Utsu (1961) has published an synthetic paper on the studies.

The present stage of studies is getting into the discussion on the change in numerical values of parameters. Miyamura (1962) discussed the difference in the value of  $b$  and its relation to the geological feature of seismic regions, although some statistical ambiguity is still left open to question according to the present authors' opinion. Suyehiro and others (1964) discussed the variation of  $b$  for fore- and aftershocks. Utsu (1961) studied the relation between the values of parameters in magnitude and time distributions.

On the other hand, not so many researches have been done on the experimental approach to the interpretation of these results. Vinogradov (1962) made a laboratory work on fracture of rocks and pointed out the parameter  $b$  depends on the properties of materials and also on the time rate of deformation. Mogi (1962a, b, c), who has made valuable experiments in this field, concluded that the parameter has a relation with the heterogeneity of material and of applied stress.

In spite of these brilliant works, many problems are not yet sufficiently solved, especially when the time, magnitude and space distribution are considered synthetically. It is of no question that the experimental study on fracture of various samples is very important to elucidate the physical meaning of results obtained in statistical seismology. In other words, if a parameter in a distribution really changes from one area to another, we should know the answer of problem that what kind of change can be estimated in what kind of property in seismic area. Otherwise many valuable results in statistical seismology are left only as a phenomenological description.

As a step of approach to the answer of this problem, the present authors undertake an experiment on microfractures of tempered glass and the results are analysed in special reference to the properties of aftershocks. The reason why the tempered glass is used as specimen will be explained later.

## 2. On material

In a few materials many secondary microfractures accompany the main fracture without any additive external force, in a similar manner to the main and aftershock sequence in natural earthquake. Rock samples of small size sometimes show the same phenomenon, although the number of secondary fractures is usually small. When melted pine resin is cooled on a metal vessel, many microfractures naturally occur. The tempered or pre-stressed glass is one of the material of this kind. Many secondary fractures take place after the tempered glass is broken down by an external force, while these secondary fractures do not occur in the case of ordinary glass. These examples may suggest that the occurrence of secondary microfractures, or aftershocks in natural earthquake, is essentially controlled by the stress distribution in the medium before the main fracture. In order to elucidate the relation between the stress and the properties, especially the statistical ones, of secondary fractures, an experiment is

carried out in this study, taking the tempered glass as material. The glass is obviously much different in its nature from the materials in earth's crust or mantle where the actual earthquakes take place. However, this experiment may still give an important clue to the understanding of occurrence of aftershocks, especially when the results are considered together with the similar results by other authors (e.g. Mogi, 1962b).

When a plate of glass is in a high temperature, say  $500^{\circ}\text{C}$ , the interior of glass should be free from the stress because it is in a low viscous state. Then the glass is cooled by air rather rapidly and the surface of plate is solidified, while the interior is still viscous because of low thermal conductivity. Since the solidified surface acts so as to prevent the contraction due to the cooling of interior, a tensile and compressional stress are produced in the interior and surface respectively. This state is fixed even after the whole plate is solidified. The tempered glass thus manufactured, therefore, is in the pre-stressed state, i.e., it has an compressional stress near surface and tensile one in the interior. The neutral state usually exists at  $0.56C$  from the center of the plate, where  $C$  denotes the half thickness of the plate. As the compressional stress near surface serves to prevent the growth of the Griffith crack that exists near surface of a plate, the mechanical strength of tempered glass is five to seven times high in comparison with that of ordinary window glass, and this is the main reason why this sort of glass is commercially manufactured.

Three kinds of tempered glasses are adopted in our experiment according to the magnitude of stress accumulated in it. These are tentatively called in this study high, medium and low states of stress for the convenience of description. These glasses are specially manufactured by the Asahi Glass Co., whose assistance is highly acknowledged. The absolute values of compressional and tensile stresses in these three kinds of glasses are given in table 1. These values are measured by the Asahi Glass Co. for a couple of samples. Although these values may fluctuate for each sample, the variance of surface compressional stress for high stress state, for example, is reasonably estimated to be less than  $0.5 \times 10^9$  dyne/cm<sup>2</sup>.

Table 1

	compression	tension
high	1.10	0.55
medium	0.97	0.45
low	0.73	0.33

( $\times 10^9$  dyne/cm<sup>2</sup>)

The stress distribution in the interior of glass cannot be directly measured. The theoretical estimation with the measured stress gives Fig. 1 for each of three kinds of glasses. In later discussions of this study the value of compressional stress on the surface is taken as a measure representing the magnitude of accumulated stress. The stress distribution near edge or corner of sample may be comparatively disturbed from that shown in Fig. 1. The effect of this disturbance near edge or corner is sometimes

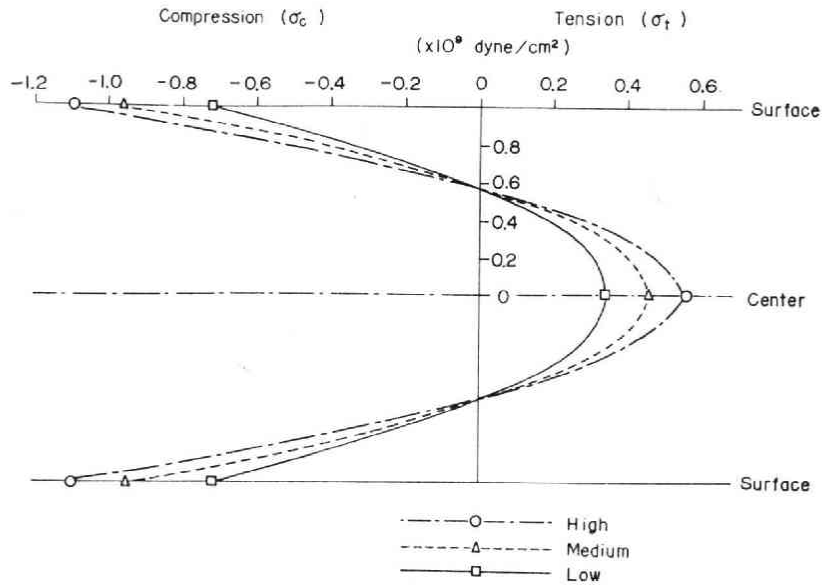


Fig. 1: Stress distribution in tempered glass.  $\circ$ ,  $\triangle$  and  $\square$  represent measured values for the glass of high, medium and low stress respectively. Lines are drawn according to the theoretical consideration.

observed in our experiment.

### 3. Experimental procedure

As stated previously, three kinds of tempered glasses, i.e., high, medium and low stressed ones, are adopted in this experiment. Most of the samples are of square form with  $30 \times 30 \times 0.5$  cm in dimension, while the plate of  $45 \times 45 \times 0.5$  cm is used in some cases. The plate is densely backed with cellophane tape to prevent the scatter of fractured blocks and to keep the crack pattern.

Initiation of main fracture is made by two different methods. One is to apply an impact by a notch-wedge at the center of plate. This method, however, is not always satisfactory for our purpose, because the magnitude of impact is hardly kept constant in each experiment. The second method is to apply a thermal stress on the surface of glass. After a scratch of about 1 cm long is made by glass cutter, the heat is supplied for a short time at the end of scratch by an electric heater. The measured variation of temperature on the surface of glass in the course of this process is seen in Fig. 2. During the process of heating up, the compressional stress due to heating acts to prevent the fracture, but the tensile stress in cooling state triggers the fracture. The crack pattern thus generated has a little complicated form, as will be stated in the next paragraph. But the condition of initiation of main fracture can be kept nearly constant. Hence most experiments are carried out by means of the second method except for the early stage of experiment.

Many secondary microcracks follow the main fracture without any additive

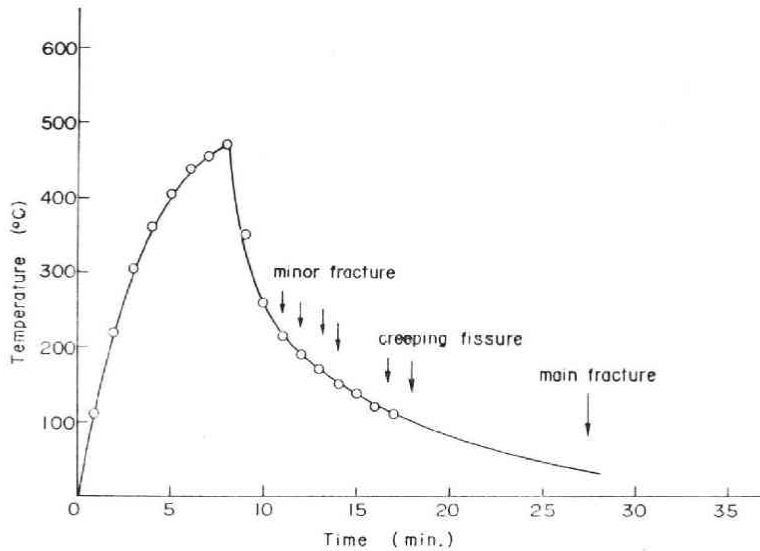


Fig. 2: Variation of temperature and its relation to the occurrence of the main fracture, when the main fracture is triggered by heating.

force, analogously to the main and aftershock sequence in natural earthquake. These secondary fractures last for several hours at the most, the duration being dependent on the magnitude of pre-existing stress.

The microcracks generate both elastic waves in the plate and acoustic waves in air. The detection of elastic waves is not so feasible as that of acoustic waves, because many cracks attenuate the wave amplitude during the course of propagation. The acoustic waves, therefore, are observed in this experiment, although the observation of elastic waves will be made in the next stage of experiment and will be reported in a future paper.

The detection of sound waves is made by a dynamic microphone F-3B, of which the output is amplified and recorded on a magnetic tape. The transmission band of high sensitive amplifier used is 1~20 kcps and the running speed of the magnetic tape is 19 cm/sec. The signal played back with a half speed of run is recorded by MR-102 type electromagnetic oscillograph whose vibrators have a natural frequency of 6 kcps. An oscilloscope having a flat response between 1~300 kcps is used as a monitor both in recording and play back. This is also available for the study on detailed form of waves by taking photographs. The measured characteristics of this monitoring system shows that the response is sufficiently flat in the frequency range of 1~10 kcps. The schematic illustration of experiment and recording system is given in Fig. 3, and the overall frequency response of recording system is seen in Fig. 4, which indicates that the response is nearly flat in the frequency range of 5~8 kcps.

A typical wave form taken by the monitor oscilloscope is given in Fig. 7 which demonstrates the form is somewhat like a damping oscillation having the duration of about 5 milliseconds. The predominant frequency is plotted in Fig. 5 against the

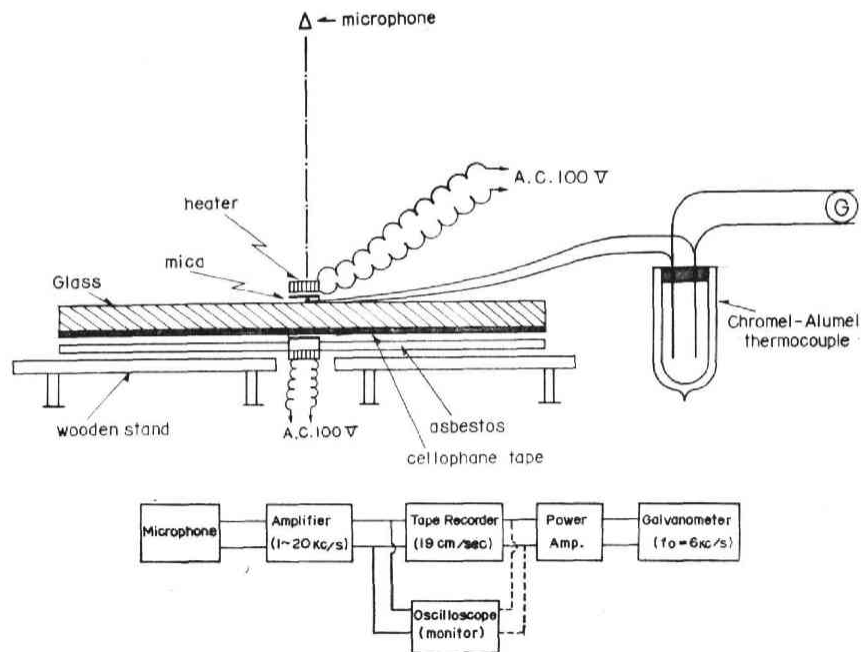


Fig. 3: Illustration of experimentation and recording system.

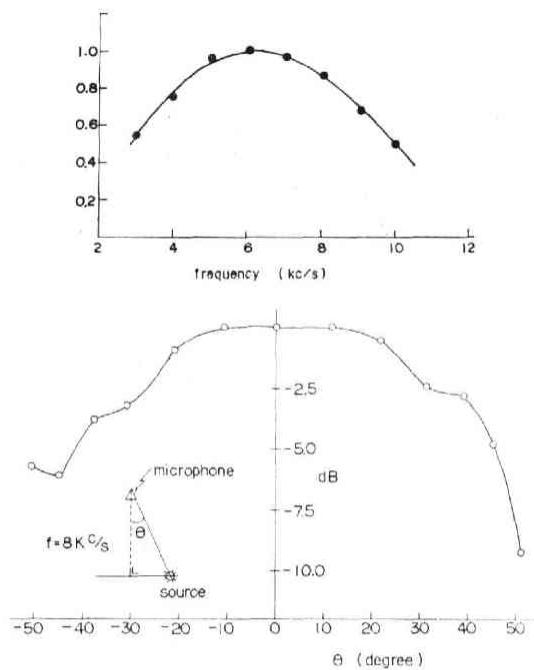


Fig. 4: Overall frequency response and measured directivity of microphone.

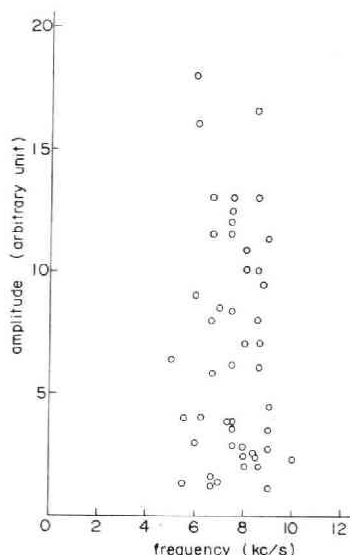


Fig. 5: Relation of the maximum amplitude and its predominant frequency of sound waves.

maximum amplitude in ordinate. This figure shows that the predominant frequency lies between 5~9 kc/s irrespective of maximum amplitude and that our recording system with the response shown in Fig. 4 is taken to be appropriate. Calibration of gain of amplifier is made in every observation using the frequency of 7 kc/s. Time marks are given in every minute overlapping the signal. An example of records is seen in Fig. 6.

The directivity of microphone is also calibrated, the result at 8 kc/s being given in Fig. 4. The pick up is always set just above the center of specimen and the distance between pick up and specimen is taken so that the solid angle of the specimen from pick up is less than  $80^\circ$ . For example, the distance is 25 cm when the size of plate is  $30 \times 30$  cm. The directivity shown in Fig. 4, therefore, is not necessarily taken into account even in the case of study of amplitude distribution.

The observation is made in the midnight in order to avoid the noises, and the experiment is carried out in the room temperature and humidity. Although the control of humidity might be necessary to get more accurate result, it will be done in future stage.

#### 4. Crack pattern

The pattern of cracks due to fracture depends on the method of initiation of main fracture and on the grade of pre-existing stress. When the fracture is triggered by a mechanical impact of notch-wedge, the crack pattern is rather regular and symmetric with respect to the impact center, as seen in Fig. 8 (a) and (b). The main fracture begins with several radial cracks starting from the point of impact and then bifurcation occurs forming transverse cracks. This is the initial stage of fracture or main



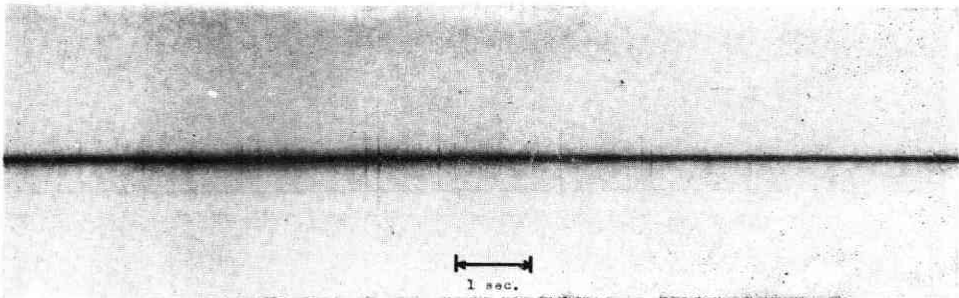


Fig. 6: Example of records in initial stage of secondary fracture. Vertical lines show the sound pulses generated by fractures.

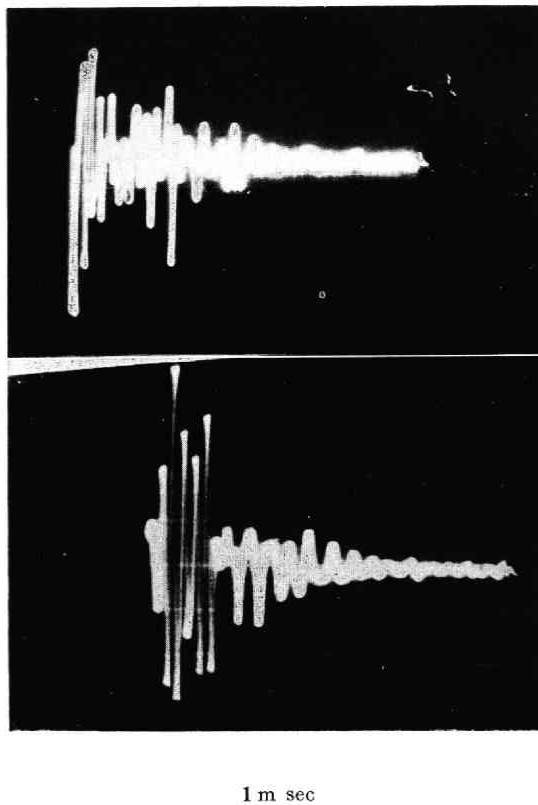


Fig. 7: Record of sound pulse detected by monitor oscilloscope.

fracture. After this stage ends within some ten milliseconds, secondary minor cracks take place and last for a duration from several ten minutes to several hours. The secondary microcrack seldom crosses over the cracks already made. It is interesting that the bifurcation rarely occurs before the radial cracks reach at some distance from the center and consequently the center part of the plate is occupied mainly by radial cracks, as clearly seen in Fig. 8 (a) and (b). Very few secondary microcracks (after-shocks) take place in this center part. The size of this part seems to depend on the magnitude of impact force and also on the grade of pre-existing stress in the glass

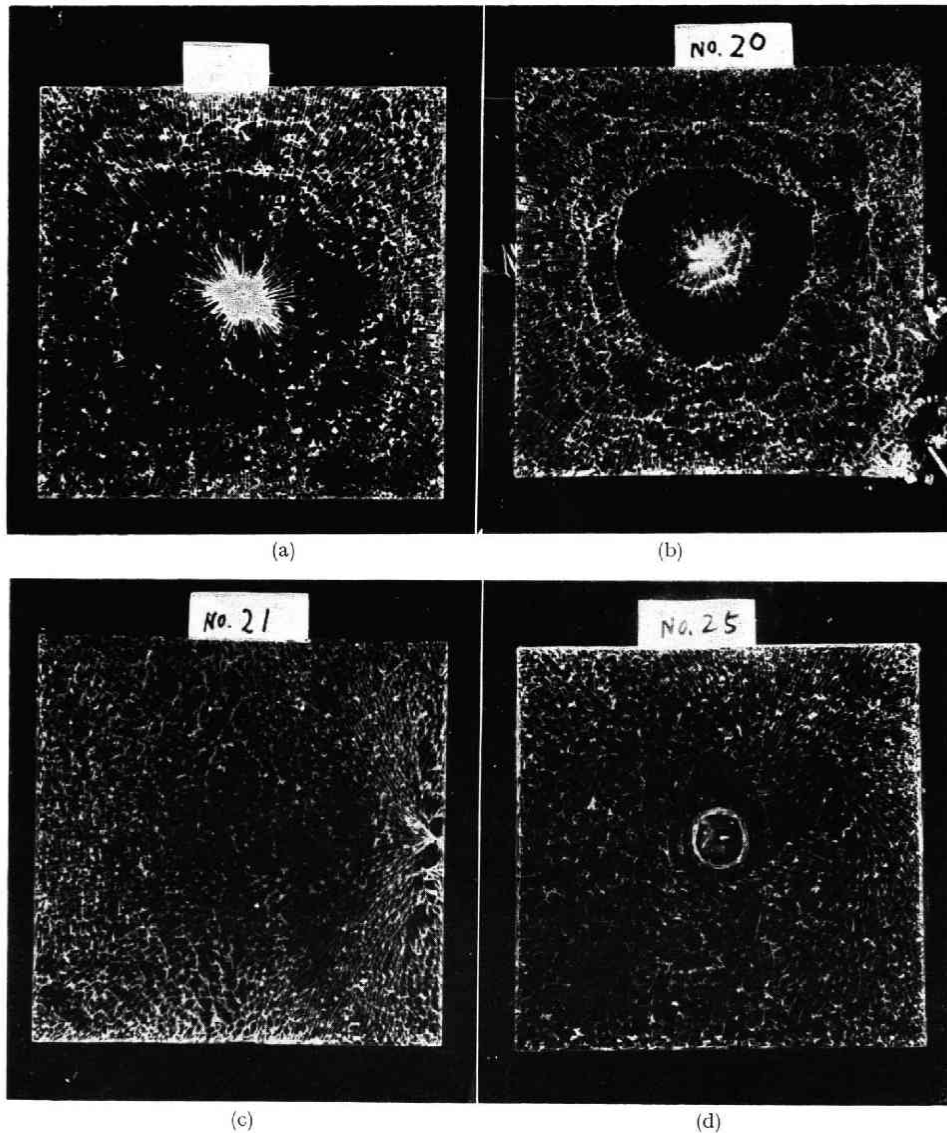


Fig. 8: Various crack patterns for high stress state.

- (a) The case where the main fracture is triggered by mechanical impact.
- (b) The case where the mechanical impact force is strong.
- (c) The case where the fracture originates at the edge of plate. The center of right side is the starting point.
- (d) The case where the main fracture is thermally triggered.

plate. But a clear relationship is hardly obtained in this experiment.

In some cases the starting point of cracks does not coincide with the center of impact but the cracks start at a point at the edge of plate. A feature of this case is that the pattern is irregular and complicated and most bifurcations occur extremely near the starting point, as seen in Fig. 8 (c). A similar phenomenon has been pointed out by

Taguti (1931) for the fractures of pine resin, when the melted resin is cooled in a metal vessel.

When the main fracture is generated by a thermal stress, the crack pattern is considerably different from that in the case of mechanical impact. In the first stage a spiral crack takes place starting at one end of the scratched flaw. After a moment, bifurcations occur at some point of the spiral crack. Hence these cracks do not show the radial pattern. The transverse cracks occur even in the center part in this case, as is shown in Fig. 8 (d). Small cracks with complicated pattern are generally seen near the edge or corner, where the stress distribution may be presumably irregular. These

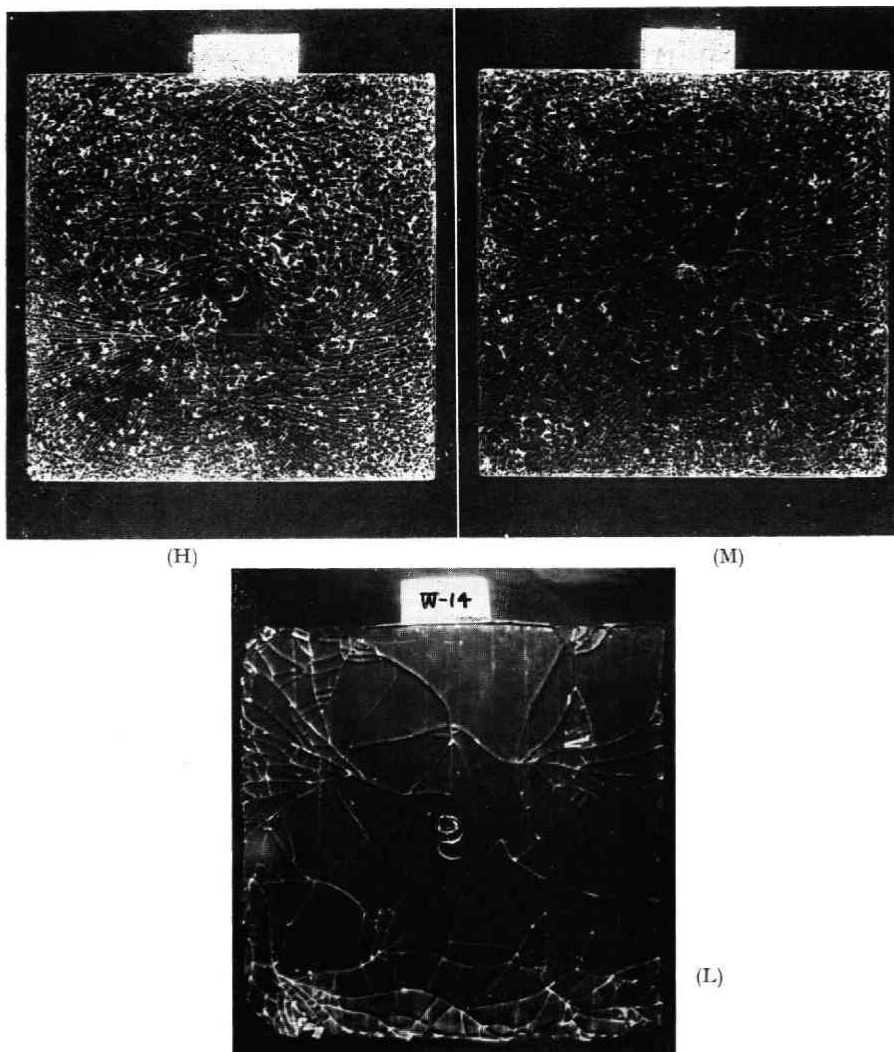


Fig. 9: Crack patterns for high (H), medium (M) and low (L) state of pre-existing stress, when the main fracture is thermally triggered.

cracks near edge or corner are frequently inclined against the surface so that these parts are liable to be taken as white parts on photographs, the examples being seen in Fig. 8.

It should be noted that the crack pattern varies much according to the grade of stress in the glass plate. As seen in Fig. 9, number of cracks increases with the magnitude of stress and the pattern becomes more complicated as the stress is greater. This circumstance apparently reflects on the magnitude and time distributions of secondary fractures, as will be studied later.

### 5. Magnitude distribution of microcracks (I)

It is well-known that the magnitude distribution of earthquakes is expressed by Gutenberg-Richter's (1949) formula,

$$\log N(M) dM = (c - bM) dM, \quad (1)$$

where  $N(M)$  is the number of earthquakes with the instrumental magnitude between  $M$  and  $M + dM$  and  $c$  and  $b$  are constants. On the other hands, the distribution of trace amplitudes is known to be represented by the so-called Ishimoto-Iida's (1939) relation,

$$n(a) da = k a^{-m} da, \quad (2)$$

where  $n(a)$  is the number of earthquakes of which the amplitudes are between  $a$  and  $a + da$ . Suzuki (1953) has proved that this relation is identical with the Gutenberg-Richter's formula and the coefficient  $b$  in (1) is connected with  $m$  in (2) as

$$b = m - 1. \quad (3)$$

The numerical value of  $b$  has generally been thought to be constant irrespective of magnitude and seismic area, although Tsuboi (1952), Miyamura (1962) and others

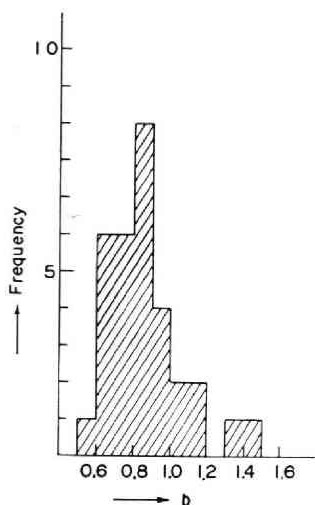


Fig. 10: Frequency distribution of value of  $b$  in the magnitude distribution for aftershocks in and near Japan and some other regions. (The data are after Utsu (1961))

have discussed the variation of  $b$  in relation to the geological feature of seismic area. Suyehiro (1966) also discussed the change in numerical value of  $b$  for foreshocks and aftershocks. Utsu (1961) summarized the magnitude distribution of aftershocks in and near Japan and some other regions. He found the value of  $b$  lies between 0.5 and 1.5, as is represented in Fig. 10.

Under these circumstances, it is very interesting and important problem to find the physical meaning of the value of  $b$ . In other words, what kind of physical property of seismic area does control the value of  $b$ . As a mean to solve the problem, we study the magnitude distribution of secondary microcracks accompanied the fracture of tempered glass, referring to the case of natural earthquakes.

The distribution of Ishimoto-Idia's type (2) is adopted in this paper. The trace amplitude on oscillogram is proportional to the intensity or accerelation of sound waves but it does not make any bias in conclution, because the predominant frequency is independent of amplitude as shown in Fig. 5. The number of microcracks having the maximum trace amplitude larger than 0.2 cm is classified into several classes according to the magunitude of amplitude. The number of class is determined by the Struges' criterion,

$$n = (1 + \log N) / \log 2$$

where  $N$  is the total number of cracks.

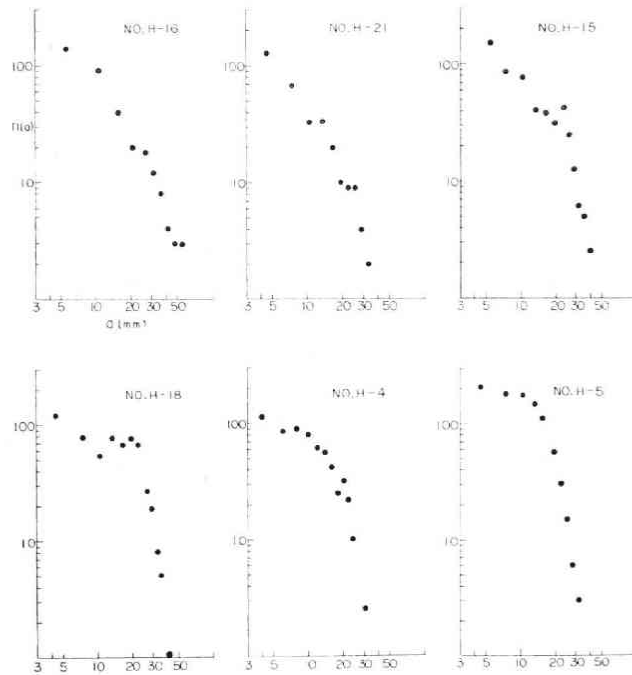


Fig. 11: Amplitude distribution when the main fracture is triggered by mechanical impact. No. H-16 and H-21 correspond to the case where the fracture originate at a different point from the impact.

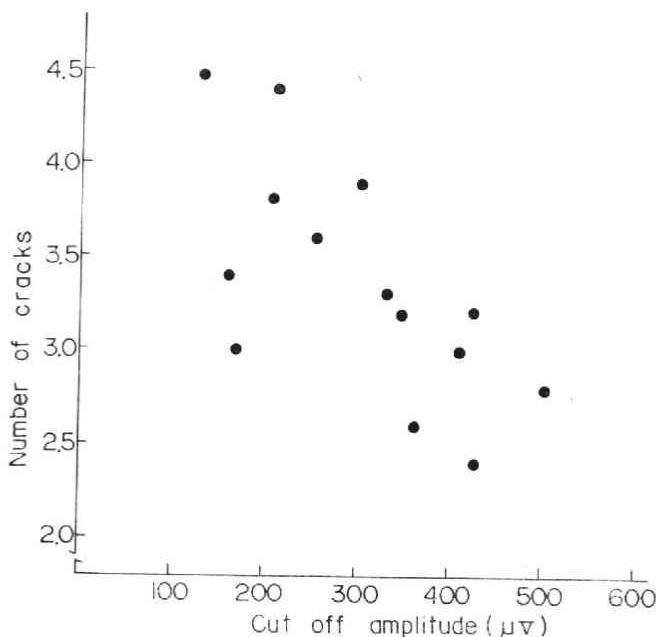


Fig. 12: Cut-off amplitude against number of radial cracks per 10 degrees on the circle with 3.9 cm in radius.

The number of cracks  $n(a)$  with amplitude between  $a$  and  $a+da$  is plotted on a doubly logarithmic diagram, of which some examples are shown in Fig. 11. If the plots are represented by a straight line, the Ishimoto-Idia's relation (2) holds good, as is the case of natural earthquakes.

It is frequently seen in the present experiment, however, that the distribution is not expressed by a single straight line but by two lines, as obviously seen in the cases of H-4, H-5 and H-18 in Fig. 11. In order to represent the feature of this type distribution, we will take the crossover point of two lines and the corresponding amplitude is tentatively called cut-off amplitude in this paper, and discuss the relation between the cut-off amplitude and some properties of fracture.

It is easily found that the cut-off amplitude is closely connected with the pattern of cracks. The number of radial cracks from the point of mechanical impact to generate the main fracture is adopted to represent the feature of crack pattern. The relation of cut-off amplitude and the number of radial cracks is seen in Fig. 12, the number being measured on the circle with 3.9cm in radius from the center of impact. The decrease of cut-off amplitude with the increasing crack number is clearly seen in Fig. 12. Since the number of radial cracks increases with the magnitude of impact force according to Shardin (1959) and Taguchi (1931), it may be said that the larger cut-off amplitude, the larger the impact force generating the main fracture. When the main fracture started at a different point from the point of impact, the amplitude distribution is well expressed by a single line, as seen in the cases of H-16 and H-21 in Fig. 11. In such cases, the cut-off amplitude may be reasonably thought to be so big that the observation can hardly show the cut-off.

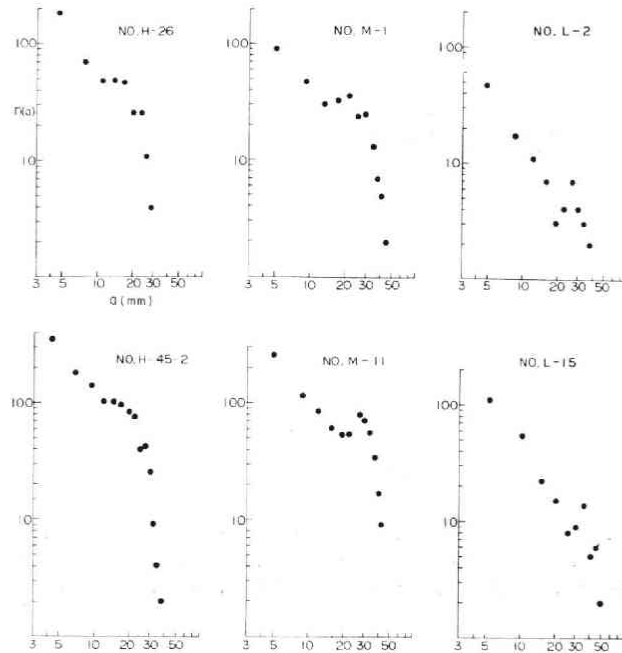


Fig. 13: Amplitude distribution of microfractures in high (H), medium (M) and low (L) state of pre-existing stress. Sudden decrease in number corresponds to cut-off.

The magnitude distribution is also dependent on the magnitude of stress stored in the glass specimen before fracture. In order to avoid the effect of magnitude of impact force on the distribution, we treat hereafter exclusively the cases where the fracture is triggered by a thermal stress. In such cases the radial cracks are not clearly seen as stated previously (See Fig. 9). However in many cases, especially when the stored stress is large, i.e., "high state", the cut-off is frequently seen, while the magnitude distribution for specimen in "low state" is mostly expressed by the Ishimoto-Iida's relation. The cut-off amplitude is found to be closely related with the stress stage, as is qualitatively seen in Fig. 13. Vinogradov (1962) found the cut-off phenomenon based on his experiment on fracture of rock samples. He stated that the cut-off is due to the effect of sample size. However the size of glasses in our case is the same for the three kinds of stress but the cut-off amplitude varies clearly depending on the stress stage. Fig. 14 demonstrates the relation taking the cut-off points in all experiments in abscissa and the surface compression in ordinate as a measure of magnitude of stored stress. The unit of amplitude in this figure is expressed by the output voltage of microphone and the cases where the Ishimoto-Iida's relation holds are plotted at the right hand end. Although the plots are rather scattered, it is evident that the cut-off amplitude increases with decreasing stress. In other words, the weak concentration of stress in specimen acts so as to elongate the range in which the magnitude distribution is well expressed by the Ishimoto-Iida's relation. The scatter of cut-off amplitude in our experiment is presumably due to the non-uniformity of humidity in part, as will be discussed later.

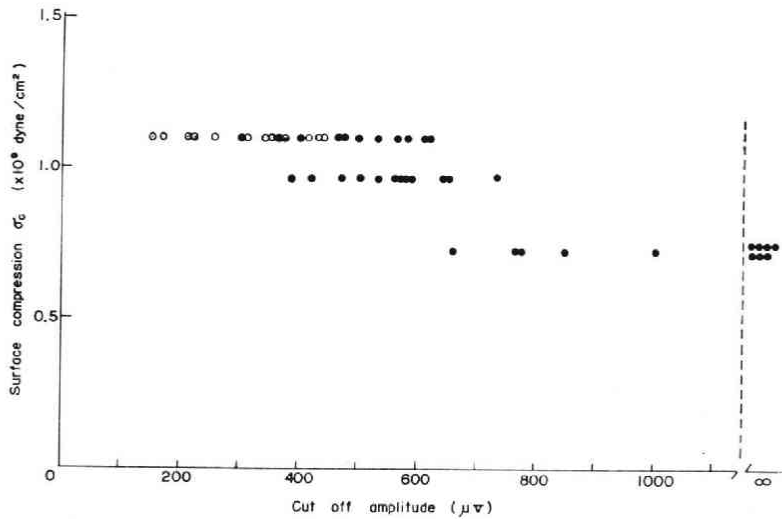


Fig. 14: Cut-off amplitude versus grade of pre-existing stress. The plots at right end indicate the case where no cut-off is observed. Hollow and solid circles represent the cases where the main fracture is triggered by mechanical and thermal forces respectively.

We will try to avoid this defect in the next stage of experiment to find a more definite relationship between cut-off amplitude and stress.

## 6. Magnitude distribution of microcracks (II)

As stated in the previous paragraph, the Ishimoto-Iida's relation does not always hold especially for specimen of high stress. The variation of magnitude distribution with respect to time is now considered. The change in distribution for high stress specimen of H-22 is shown in Fig. 15. The distribution in early stage of secondary fractures is well represented by a straight line. According to the lapse of time, however, the distribution becomes to indicate an upward concave feature and turns out to show the cut-off. This means that the microcracks having a specified amplitude occur with a higher probability in the later stage than that in early stage. Hence the model of occurrence of secondary fractures changes at a time after main fracture. To elucidate this circumstance, the cumulative value of amplitudes of microcracks is calculated as a function of time, the results for high, medium and low stress glasses being seen in Fig. 16. This procedure is based on a similar consideration to the Benioff's study (1951) concerning actual aftershocks, though the released strain was adopted in his study instead of amplitude. This difference between amplitude and strain is not essential for our purpose and the amplitude is taken simply because of convenience. It is clearly seen in Fig. 16 that the cumulative amplitude is well expressed by two straight lines with respect to time and crossover may reasonably divide the early and later stage of secondary fractures. The values of crossover are approximately 1~2, 2~4, 3~9 minutes after the main fracture respectively for high, medium and low stress glasses. The total microcracks are then divided into two groups, i.e., those in early and later stages and the



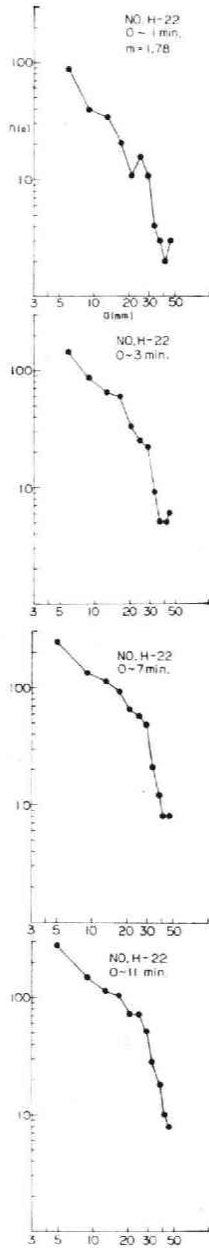


Fig. 15.

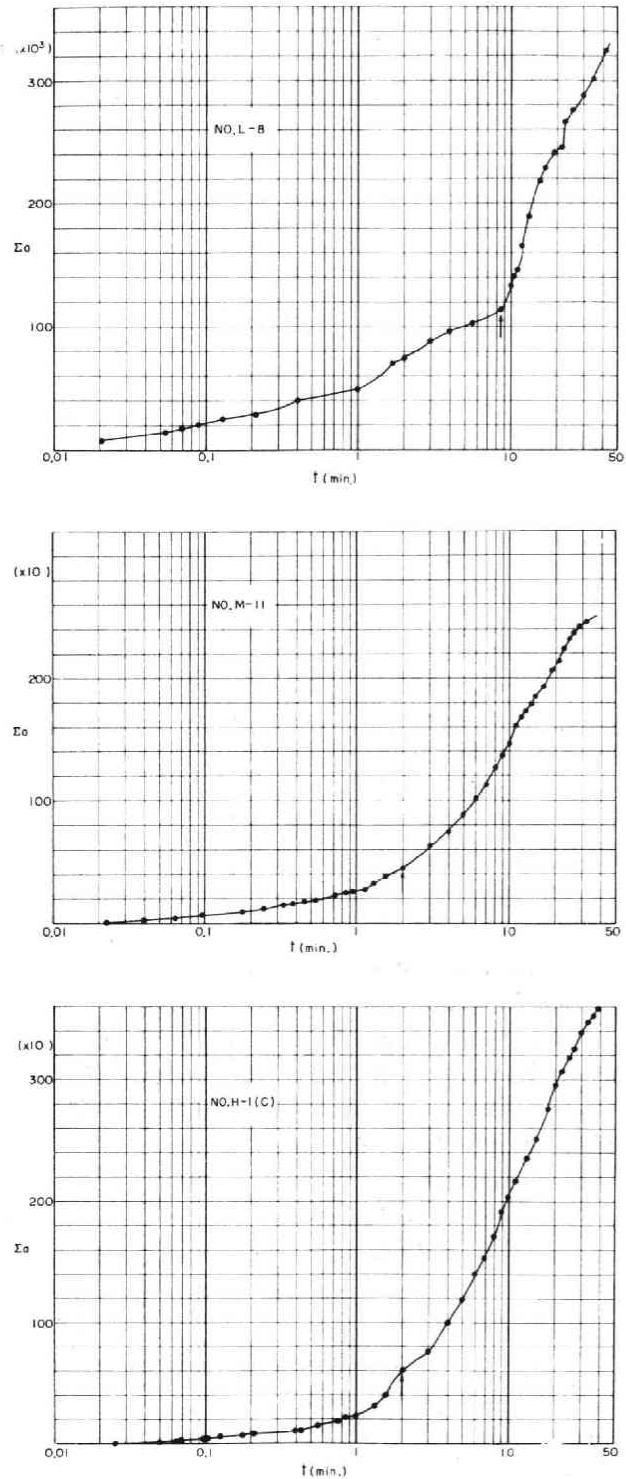


Fig. 16.

Fig. 15: Variation of magnitude distribution with lapse of time.

Fig. 16: Variation of cumulative amplitude against time (time dependence of energy release) in cases of high, medium and low stress. Arrows indicate the points of conversion from earlier to later stage.

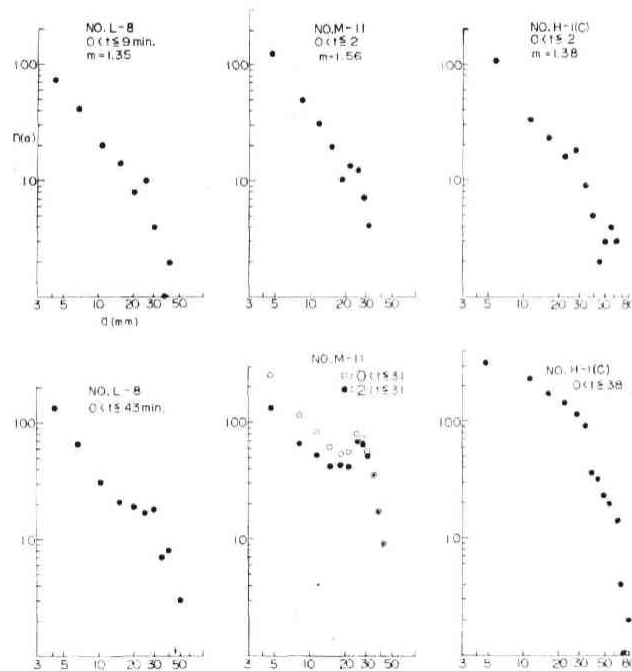


Fig. 17: Amplitude distribution of microcracks. Upper half represent those in earlier stage and lower half is for whole data. In No. M-11, the distribution in later stage is also shown by solid circles.

magnitude distribution for each group is constructed. Fig. 17, which shows some typical examples, indicates an interesting fact that the magnitude distribution in early stage is well represented by the Ishimoto-Iida's relation irrespective of magnitude of stored stress. The value of  $m$  in Eq. (2) is between 1.3 and 1.8, which is a little smaller than that for natural earthquakes.

In later stage, however, the magnitude distribution is much different from the Ishimoto-Iida's relation. Since the duration of early stage is shorter as the stored stress is greater, the discrepancy of distribution of total microcracks from the Ishimoto-Iida's relation is larger for higher stress glass. This is compatible with the result in previous paragraph.

Consequently the following conclusions are obtained. The occurrence of secondary fractures consists of two modes of fracture, although the nature of difference between the two modes is not elucidated at this moment. The transition from the first to the second mode takes place at a specified time after the main fracture, the specified time being dependent on the magnitude of stored stress. The magnitude distribution of secondary cracks in the first stage follow the Ishimoto-Iida's relation having the value of  $m$  around 1.5, but that in the second is much different.

This kind of change in magnitude distribution according to lapse of time has never found in the case of natural aftershocks. The duration of the first stage in actual

earthquakes, therefore, is thought to be long enough so that the number of aftershocks in the second stage is too few to be recognized in statistical study. This is to say that the stress stored in actual seismic area is not so large in comparison with the high stress specimen in our experiment.

### 7. Time distribution of microcracks

The time distribution of aftershocks is one of the most frequently discussed problems in statistical seismology. Omori (1894) found the famous hyperbolic formula,

$$n(t) dt = \frac{B}{t+A} dt, \quad (4)$$

where  $n(t)$  is the number of aftershocks at a time interval  $t \sim t+dt$  after the main shock and  $A$  and  $B$  are constants. Utsu (1961) generalized this formula into

$$n(t) dt = \frac{A}{(t+C)^p} dt, \quad (5)$$

which is valid in most cases. The values of  $p$  in various cases are obtained to be between 1.0 and 1.4 and  $C$  usually has a smaller value than 1 day. Hence the form as

$$n(t) dt = A \cdot t^{-p} dt \quad (6)$$

has been also successfully used by many authors (Senshu (1959), Utsu (1961) and Mogi (1962d)). Mogi (1962d) discussed the geographical distribution of the numerical

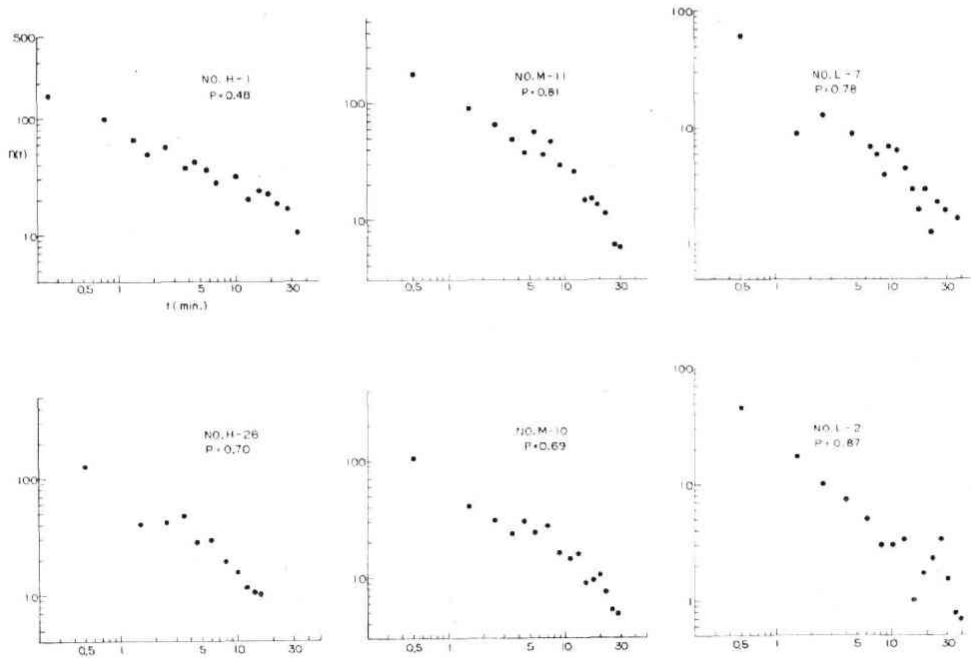


Fig. 18: Time distribution of microfractures for high (H), medium (M) and low (L) state of pre-existing stress.

value of  $p$  in and near Japan and Utsu (1961) studied the relation between the magnitude and time distribution of aftershocks. Taking these into consideration, we will discuss the time distribution of secondary fractures in our experiments. Examples of the distribution are seen in Fig. 18, which indicates the time distribution in every case is well represented by a straight line in doubly logarithmic diagram. The phenomenon of cut-off is seldom in time distribution. This implies the formula

$$n(t) dt = A t^{-p} dt \quad (6)$$

holds good in our case. The value of  $p$  is apparently smaller than unity so that the simple Omori's formula (4) is not the case of the present experiment irrespective of the grade of stored stress. The time interval  $dt$  is taken to be one minute in most cases. However the mean value of  $n(t)$  for successive two or three minutes is sometimes adopted when  $t$  is larger than ten minutes, in order to avoid the zero value of  $n(t)$ .

The value of  $p$  for high, medium and low stress are given in Fig. 19, the surface compression being taken as the measure of grade of stress in ordinate. Although the values scatter considerably, it is clear that the value of  $p$  decreases with increasing stored stress.

Acloque and Morain (1963) also studied the number of secondary fractures of tempered glass from some different point of view. Using a circle plate of glass, of which the radius is 30 cm and the thickness is 5.7 mm, they found the number of cracks is much influenced by the humidity around the specimen. Their result is reproduced (with a little modification) in Fig. 20, in which the cumulative number of cracks is

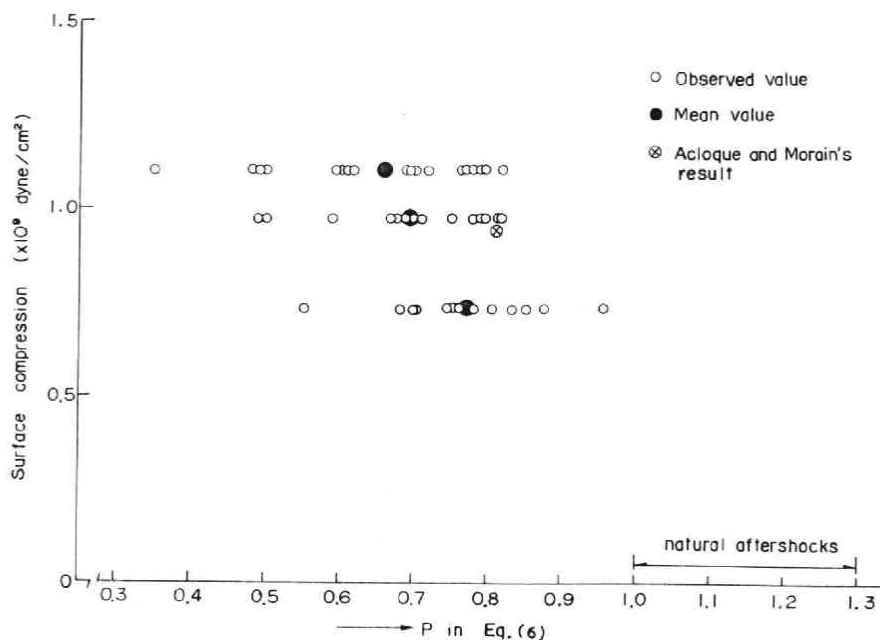


Fig. 19: Values of  $p$  in time distribution in various stress states. Acloque and Morain's result (1963) is included. Range of  $p$  for aftershocks is indicated by arrow.

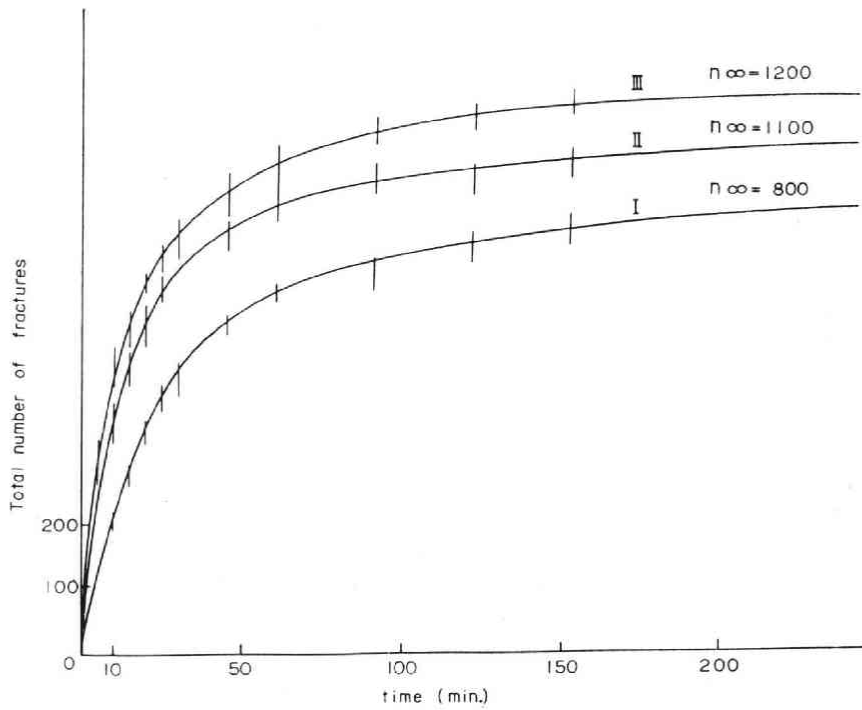


Fig. 20: Cumulative number of secondary fractures versus time lapse at three state of humidity.

I: air content 5% humidity. II: air content 40% humidity.  
 III: air content 85% humidity. (after Acloque and Morain with slight modification)

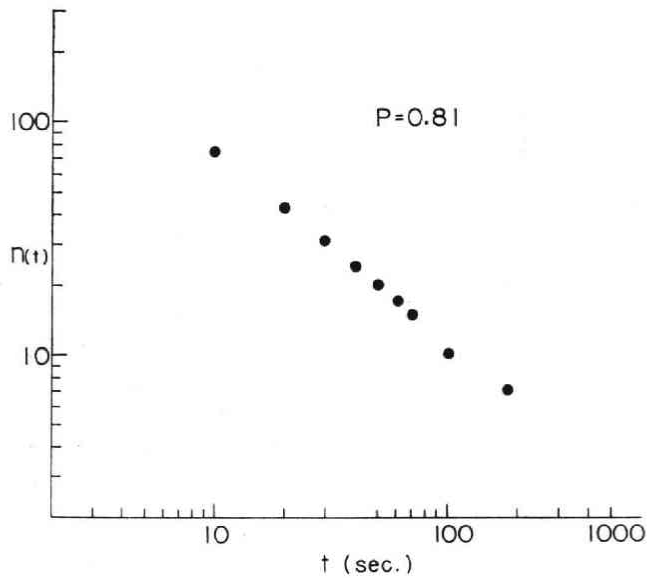


Fig. 21: Time distribution of secondary cracks calculated from the Acloque and Morain's result.

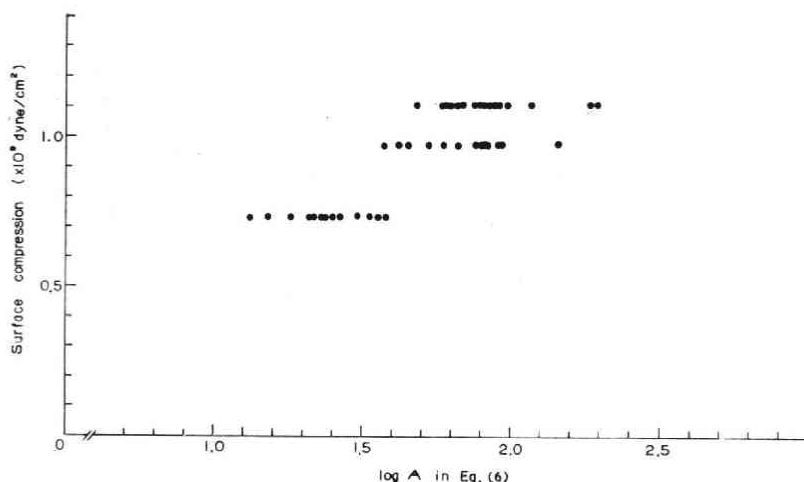


Fig. 22: Relation between the coefficient  $\log A$  in Eq. (6) and grade of pre-existing stress.

taken in ordinate. From this figure the number of cracks in a unit time is read and replotted in doubly logarithmic diagram. As seen in an example shown in Fig. 21, the data by them are also well expressed by the same distribution as that in the present study. The value of  $p$  varies by a small amount according to the change in humidity, though a definite relation is hardly obtained because of scanty of data. This fluctuation due to humidity may be one of the reasons why the values of  $p$  in our experiment scatter so much. This may be also the case in magnitude distribution, as was stated before. The value of  $p$  based on Aclouque and Morain's data is included in the plots in Fig. 19 with a different symbol.

The numerical values of  $p$  in the experiment lie between 0.4 and 0.9. This is a little smaller than the values for actual aftershocks. Since  $p$  decreases with increasing pre-existing stress, the larger value of  $p$  for aftershocks indicates that the stress accumulation in actual seismic area may correspond to the lower stress state than that of low stress glass used in this experiment. This conclusion is fairly compatible with that from magnitude distribution.

The values of  $A$ , which is the number of cracks at  $t=1$ , is shown in Fig. 22, which implies the increasing  $A$  with the grade of stress.

## 8. Discussions

It has been discussed that the cut-off amplitude in magnitude distribution and the value of parameter  $p$  in time distribution are closely connected with the pre-existing stress. Some quantitative comparison of the result of experiment with the property of actual seismic area is now made. As stated before, the value of  $p$  for aftershocks is obtained by Utsu (19961) to be between 1.0~1.4 in many cases. We take the mean value of  $p$  for each stage of stress. The mean values for high, medium and low states are plotted in Fig. 19 by the symbol of solid circle. From this figure we can extrapolate the surface compressional stress corresponding to the value of  $p$  for aftershocks. The

value thus obtained is of the order of  $10^7$  dyne/cm<sup>2</sup>, which is smaller than the breaking stress of tempered glass by the factor of  $10^{-3}$ .

On the other hand, Chinnery (1964) estimated the strength of seismic area under horizontal shear stress based on the study of five earthquakes which accompanied the surface faults. He concluded that the large fault of strike slip type occur with the stress smaller than  $10^7$  dyne/cm<sup>2</sup>, and this value is smaller than the generally accepted value of breaking point of earth's crust by the factor of  $10^{-2}$ . The magnitude of stress accumulation in whole seismic area or the so-called aftershock region is reasonably estimated to be smaller than this value by a factor of  $10^{-1}$  or  $10^{-2}$ , considering the result of geodetic observations of land deformation in the case of occurrence of big earthquake. The coincidence of the both results by Chinnery and our experiment is of some interest, although it might be dangerous to correspond these two results directly neglecting the big difference in nature of materials in two cases.

The circumstance that the stress accumulation in aftershock field is far less than the breaking point by the factor of  $10^{-3} \sim 10^{-4}$  also fairly explain the fact that the cut-off amplitude is scarcely seen in actual earthquakes, as is easily accepted from the relation in Fig. 19. It should be noted here that the Griffith's theory (1920) on brittle fracture may be helpful from various view points to the understanding of mechanism of aftershock occurrence, if they occur in the field of stress which is rather weakly accumulated.

## 9. Summarized conclusions

The conclusions of this study are summarized as follows.

- 1) An experiment on secondary fractures of tempered glass is made and the statistical properties of fractures are compared with those for natural earthquakes.
- 2) Frequency distribution of amplitudes is not always follow the Ishimoto-Iida's relation but a cut-off is frequently seen. The cut-off amplitude increases with decreasing pre-existing stress.
- 3) A change in mode of fracture takes place at a time in the course of occurrence of secondary fractures. In the earlier stage the Ishimoto-Iida's relation holds good, while the distribution with cut-off appears in the later stage. Time of mode conversion above mentioned is later for lower stress state.
- 4) The decrease in number of secondary fractures with lapse of time is well represented by the generalized Omori's formula, which holds in most cases of aftershocks. The value of parameter  $p$  in the formula is smaller for tempered glass used than that for aftershocks, and the value increases with decreasing stored stress.
- 5) The number of secondary fractures increases with increasing stress.
- 6) Comparison of these results with studies on natural aftershocks gives the inference that the accumulation of stress in actual seismic area is lower than that in low stress state of our material.
- 7) Crack pattern changes according to the stress state and also to the method of initiation of main fracture. Initiation by thermal stress gives a better result for our purpose especially in keeping the same condition of fracture.

8) The estimation of stress accumulation for aftershock field from our experiment gives an interesting figure of stress ratio to the breaking strength, if it may be directly compared with the value obtained from seismic result.

In conclusion the writers wish to express the acknowledgements to Dr. A. Takagi for his valuable suggestions and discussions. Their hearty thanks are also due to the Asahi Glass Co. who kindly prepares the materials of special state of stress especially for our experiment.

A part of this work is financially supported by the Ministry of Education of the Japan Government as the Personal Research Project.

#### REFERENCES

- Acloque, P. and M. Morain, 1963: La fatigue statique du verre étudiee à partir de la fragmentation secondaire dans le verre trempé. *Silicates Industriels* 411-415.
- Benioff, H., 1951: Earthquakes and rock creep, Part I. *Bull. Seis. Soc. Amer.*, **41**, 31-62.
- Chinnery, M.A., 1964: The strength of the earth's crust under horizontal shear stress. *Jour. Geophys. Res.*, **69**, 2085-2089.
- Griffith, A.A., 1920: The phenomena of rupture and flow in solid. *Phil. Trans. Roy. Soc.*, **221**, 163-198.
- Gutenberg, B. and C.R. Richter, 1949: Seismicity of the earth. Princeton Univ. Press.
- Ishimoto, M. and K. Iida, 1939: Observations sur les séismes enregistrés par le microscismographe construit dernièrement (1). *Bull. Earthq. Res. Inst., Tokyo Univ.*, **17**, 443-478. (In Japanese with French abstract)
- Mogi, K., 1962a: Study of elastic shocks caused by the fracture of heterogeneous materials and its relations to earthquake phenomena. *Bull. Earthq. Res. Inst., Tokyo Univ.*, **40**, 125-173.
- , 1962b: Magnitude-frequency relation for elastic shocks accompanying fractures of various materials and some related problems in earthquakes (2nd paper). *ibid.* **40**, 831-853.
- , 1962c: The fracture of a semi-infinite body caused by an inner stress origin and its relation to the earthquake phenomena — The case of the materials having some heterogenous structures —. *ibid.* **41**, 594-614.
- , 1962d: On the time distribution of aftershocks accompanying the recent major earthquakes in and near Japan. *ibid.* **40**, 107-124.
- Miyamura, S., 1962: Seismicity and geotectonics. *Jour. Seis. Soc. Japan, Series II*, **15**, 23-52.
- Omori, F., 1894: On the aftershocks of earthquakes. *Jour. Coll. Science Imp. Univ., Tokyo Japan*, **7**, 111-200.
- Senshu, H., 1959: On time interval distribution of aftershocks. *Jour. Seis. Soc. Japan. Series II*, **12**, 149-161.
- Shardin, H., 1959: Velocity effects in fracture. In: Averbach, B.L. (Editor), *Fracture*. The M.I.T. Press, 297-330.
- Suyehiro, S., T. Asada and M. Ohtake, 1964: Foreshocks and aftershocks accompanying a perceptible earthquake. *Meteor. and Geophys.*, **15**, 71-88.
- Suyehiro, S., 1966: Difference between aftershocks and foreshocks in the relationship of magnitude to frequency of occurrence for the great Chilean earthquake of 1960. *Bull. Seis. Soc. Amer.*, **56**, 185-200.
- Suzuki, Z., 1953: A statistical study on the occurrence of small earthquakes, I. *Sci. Rep. Tohoku Univ., Series 5*, **5**, 177-182.
- , 1959: A statistical study on the occurrence of small earthquakes, IV. *ibid.* **11**, 10-53.
- Taguchi, U., 1931: On the propagation of crack. *Bull. Inst. Phys. Chem. Res.*, **10**, 521-605.



- Tsuboi, C., 1952: Magnitude frequency relation for earthquakes in and near Japan. *Jour. Phys. Earth*, **1**, 47-54.
- Utsu, T., 1961: A statistical study on the occurrence of aftershocks. *Geophys. Mag.*, **30**, 521-605.
- Vinogradov, S.P., 1962: Experimental study of the distribution of the number of fracture in respect to the energy liberated by the destruction of rocks. *Bull. (Izv). Acad. Sci. USSR, Geophy. Series*, (English ed.) No. 2, 119-125.